ISSN 0018-1439, High Energy Chemistry, 2009, Vol. 43, No. 2, pp. 105–115. © Pleiades Publishing, Ltd., 2009.
Original Russian Text © L.G. Samsonova, N.I. Selivanov, T.N. Kopylova, V.Ya. Artyukhov, G.V. Maier, V.G. Plotnikov, V.A. Sazhnikov, A.A. Khlebunov, M.V. Alfimov, 2009, published in Khimiya Vysokikh Energii, 2009, Vol. 43, No. 2, pp. 149–159.

PHOTOCHEMISTRY

Experimental and Theoretical Investigation of the Spectral and Luminescent Properties of Some Acridine Compounds

L. G. Samsonova[a], N. I. Selivanov[a], T. N. Kopylova[a], V. Ya. Artyukhov[a], G. V. Maier[a], V. G. Plotnikov[b], V. A. Sazhnikov[b], A. A. Khlebunov[b], and M. V. Alfimov[b]

[a] *Tomsk State University, pr. Lenina 36, Tomsk, 634050 Russia*

[b] *Photochemistry Center, Russian Academy of Sciences, ul. Novatorov 7a, Moscow, 119421 Russia*

e-mail: byzantium@list.ru

Received July 1, 2008

Abstract—Complex (experimental and quantum-chemical) investigation of the spectral and luminescent properties of acridine, 9-aminoacridine, 2,7-dimethyl-9-ditolylaminoacridine, and their protonated forms was performed. The electronic absorption and fluorescence spectra of the acridine dyes were studied at room temperature in ethanolic solutions at different pH values and in other solvents of different chemical nature and polarity. The energies of the excited states, the deactivation rate constants for the excited states, and the dipole moments are presented, which were obtained by calculations using the method of intermediate neglect of the differential overlap with special spectroscopic parameterization.

DOI: 10.1134/S0018143909020076

Optical chemical sensors that use luminescence, including changes in the radiation intensity, radiation wavelengths, spectral shape, and luminescence lifetime, possess high sensitivity and selectivity toward molecules of different analytes [1, 2]. Therefore, topical issues are a targeted search for and synthesis of compounds exhibiting sensor properties and the design of optical sensor materials on their basis [3–12].

Molecules of dyes that can be used to create optical sensor materials, have to meet a number of requirements, the most important of which is a sufficiently high optical response to the presence of analytes. Molecules of acridine dyes, in particular, 9-substituted acridine derivatives, meet this requirement [13–15]. For example, it was shown that the position of the fluorescence maximum of 2,7-dimethyl-9-ditolylaminoacridine (9-DTAA) strongly depends on the polarity of the solvent used (the bathochromic shift is about 100 nm on passing from hexane to acetone and acetonitrile) [16]. In addition, owing to the presence of a nitrogen atom in molecules of acridine dyes, these compounds are weak organic bases capable of adding a proton in acidic media. The protonated forms of these molecules can possess spectral and luminescent properties sharply different from those of the corresponding neutral forms, which increases functional capabilities of these compounds.

In this work, to analyze the changes in the spectral and luminescent properties and the character of the photophysical processes as a function of the nature of the substituent in the position 9 of acridine, we studied in detail the excited-state energies, the dipole moments of the ground and excited states, and the constants for the radiative and nonradiative processes of 9-aminoacridine (9-AA) and 9-DTAA.

Note that there is no complete understanding of the photophysical processes characteristic of this series of molecules, although acridine and its derivatives have been extensively studied [17–25]. The most controversial literature data concern the fluorescent properties of acridine in solvents of different polarity. Meanwhile, understanding the photophysical processes in acridine is very important, because it is the parent compound for the entire acridine series.

Therefore, much attention is also given in this work to quantum-chemical calculation of the characteristics of excited states and the constants of radiative and nonradiative processes in acridine, as well as interpretation of the experimental and calculated data available in the literature.

The structural formulas of the compounds in question are shown in Fig. 1.

EXPERIMENTAL

The spectral and luminescent properties of acridines were studied in ethanol, ethyl acetate, cyclohexane, and carbon tetrachloride. Before use, ethanol was purified by rectification; ethyl acetate (reagent grade), cyclohexane (reagent grade), and carbon tetrachloride (reagent grade) were used without preliminary purification. To study the spectral and luminescent properties of the cationic forms of the test compounds, their ethanolic solutions were used at a concentration of 10^{-5} mol l^{-1} with admixtures of hydrochloric acid (10^{-5}–10^{-1} mol l^{-}). Absorption and fluorescence spectra were recorded on

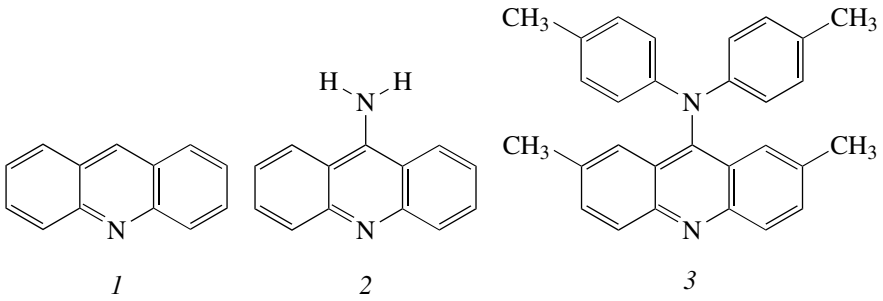

1 *2* *3*

Fig. 1. Structural formulas of (*1*) acridine, (*2*) 9-aminoacridine, and (*3*) 2,7-dimethyl-9-ditolylaminoacridine.

a CM2203 (SOLAR, Belarus) spectrofluorimeter. Fluorescence quantum yields were determined using the method of comparison with a standard [17]. Coumarin 120 in ethanol ($\varphi = 0.98$) and coumarin 153 in ethanol ($\varphi = 0.38$) and ethyl acetate ($\varphi = 0.93$) [26] were used as standards.

QUANTUM-CHEMICAL CALCULATION PROCEDURE

The quantum-chemical calculations of molecules were performed on the basis of the semiempirical method of intermediate neglect of the differential overlap (INDO) with special spectroscopic parameterization [27]. The method was developed for correct calculation of the spectral and luminescent properties of polyatomic organic molecules and was successfully used for the study of photonics of polyatomic organic molecules [28].

The wave functions of electronically excited states Ψ_p were represented as a linear decomposition into singly excited configurations $|i \longrightarrow k\rangle$:

$$\Psi_p = \sum_{ik} A_{ik}^p |i \longrightarrow k\rangle, \quad (1)$$

$$|i\rangle = \sum_{\mu} c_{i\mu} |\chi_\mu\rangle = \sum_{A} \sum_{\mu \in A} c_{i\mu} |\chi_\mu\rangle, \quad (2)$$

where $|i\rangle$ is the molecular orbital (MO) and χ_μ is the atomic orbital (AO). Summation over A means summation over AO of the atom A. The squared coefficients $|c_{i\mu}|^2$ determine the contribution of AO χ_μ to the formation (structure) of MO $|i\rangle$. As a rule, it is possible to distinguish some fragments in complex molecules with several functional groups. Then, Eq. (2) can be rewritten as the sum over these fragments:

$$|i\rangle = \sum_{k} \sum_{A \in k} \sum_{\mu \in A} c_{i\mu} |\chi_\mu\rangle. \quad (3)$$

Analysis of the structure of MO on the basis of Eq. (3) permits their classification by the degree of localization on a certain fragment (or fragments) of the molecule.

The singly excited configuration $|i \longrightarrow k\rangle$ is formed upon excitation of an electron from MO $|i\rangle$ occupied in the excited state to unoccupied (vacant) MO $|k\rangle$. It is known that in studies of aromatic and heteroaromatic compounds, from symmetry considerations, MO can be separated into π-, σ-, and *n* types. Furthermore, MO can be classified by the spatial feature. The most known type of this classification is MO of the *n* type, which mainly includes AO of a heteroatom with a lone electron pair. The concept of spatial localization of MO is used, for example, in consideration of electron density redistribution (charge transfer).

The value of $|A_{ik}|^2$ determines the contribution of the configuration $|i \longrightarrow k\rangle$ to the formation of the wave function of the excited state. Knowing the orbital nature and the spatial localization of MO $|i\rangle$ and $|k\rangle$, it is possible to classify the wave function of the excited electronic state by the orbital nature and the possible localization on a certain fragment (or fragments) of a molecule or a molecular system.

The INDO method permits calculation of the energies and the wave functions of electronic states of a polyatomic organic molecule. However, this is insufficient for investigation into the photonics of such molecules. According to Terenin's definition, photonics of molecules is a set of photophysical and photochemical processes occurring in these molecules after absorption of a quantum of light [18]. The spectral and luminescent properties of photostable organic compounds are determined by the photophysical processes, namely, electronic transitions between vibronic states of the molecule.

Electronic transitions in polyatomic organic molecules are divided into radiative and nonradiative transitions. The radiation rate constant k_r was calculated by Eq. (4):

$$k_r(S_i \longrightarrow S_0) = 2^{-1/2} f(S_i \longrightarrow S_0)\, E^2(S_i \longrightarrow S_0), \quad (4)$$

where $f(S_i \longrightarrow S_0)$ is the oscillator strength and $E(S_i \longrightarrow S_0)$ is the energy of the $S_i \longrightarrow S_0$ electronic transition.

There are two types of intramolecular interactions initiating nonradiative mechanisms of transformation (conversion, relaxation) of electronic excitation energy.

One of them is internal conversion, the nonradiative transition between different electronic states of the same multiplicity ($S_i \longrightarrow S_f$, $T_i \longrightarrow T_f$). Nonradiative electronic transition between electronic states of different multiplicity ($S_i \longrightarrow T_f$, $T_i \longrightarrow S_f$) is referred to as intersystem crossing (intercombination conversion, singlet–triplet conversion).

For quantitative determination of the rate constants for internal conversion processes in polyatomic molecules, Eq. (5) was derived on the basis of the general theory of nonradiative transitions, involving experimental data and quantum-chemical calculation results [29, 30]:

$$k_{ic}(\Psi_p \longrightarrow \Psi_q) = Q_{pq} W_{pq} E_{pq}^{-2}, \quad (5)$$

where Q_{pq} is the vibrational factor, E_{pq} is the energy of the electronic transition, and W_{pq} is the factor describing the superposition (overlapping) of the wave functions of the electronic states Ψ_p and Ψ_q. To obtain the dependence of k_{pq} on E_{pq}, the approximations at which $W_{pq} \cong 1/N_{CH}$ (N_{CH} is the number of C–H bonds), which quite firmly hold for π-electronic molecules, were used and Eq. (5) could be rewritten in the form

$$k_{pq} = Q_{pq} E_{pq}^{-2} / N_{CH}. \quad (6)$$

Thus, we established the dependence of the efficiency of internal conversion on the structure of π-electronic molecules.

To evaluate the rate constant of intersystem crossing, Eq. (7) was obtained [31, 32]:

$$k_{ST} = 10^{10} |\langle i | H_{SO} | f \rangle|^2 F_{0n}, \quad (7)$$

where i and f are the electronic wave functions of the initial and final states, respectively; H_{SO} is the one-electron operator of spin–orbit coupling; and F is the Franck–Condon factor. In the general case, calculation of the matrix elements of H_{SO} reduces to calculation of one-centered, two-centered, and three-centered integrals. The most widespread is the one-centered approximation, in which only one-centered integrals $\langle \chi_\mu^A | H_{SO}^A | \chi_\nu^A \rangle$ are taken into account. This approximation well describes the $S \rightleftharpoons T$ transitions between the states of different orbital nature ($S_{n\pi^*} \rightleftharpoons T_{\pi\pi^*}$ or $S_{\pi\pi^*} \rightleftharpoons T_{n\pi^*}$), but does not permit calculation of spin–orbit coupling between the ππ* states ($S_{\pi\pi^*} \rightleftharpoons T_{\pi\pi^*}$). However, El-Sayed's empirical rule [33] was known, according to which the value of spin–orbit coupling of the states of the same orbital type ($^1\pi\pi^* \longrightarrow {}^3\pi\pi^*$, $^1n\pi^* \longrightarrow {}^3n\pi^*$) for azaheterocyclic compounds is 2–4 orders of magnitude below that of the states of different orbital types ($^1\pi\pi^* \longrightarrow {}^3n\pi^*$, $^1n\pi^* \longrightarrow {}^3\pi\pi^*$). The generalized estimation on the basis of quantum-chemical calculations of the matrix element $\langle i | H_{SO} | f \rangle$ gave a value on the order of 10 cm^{-1} for the latter case. For spin–orbit coupling of ππ* states, only one estimation was available, 0.3 cm^{-1} for the benzene molecule [34]. These values were used to estimate $\langle i | H_{SO} | f \rangle$ in Eq. (7):

$$k_{ST}(^1\pi\pi^* \longrightarrow {}^3\pi\pi^*) = 10^9 F_{0n}\ (s^{-1}), \quad (8)$$

$$k_{ST}(^1\pi\pi^* \longrightarrow {}^3n\pi^*) = 10^{12} F_{0n}\ (s^{-1}). \quad (9)$$

Thus, in Eqs. (6)–(9) for estimation of the rate constants for internal conversion (k_{IC}) and intersystem crossing (k_{ST}), general concepts of particular types of electronic wave functions of the initial and final states were used. Actually, in both cases the dependences of the rate constant for the transition on the energy gap between the electronic states were obtained. This did not make it possible to explicitly take into account the diversity of molecular orbital nature of interacting electronic states and complicated the detailed analysis of the specifics of photophysical processes depending on the molecular structure. Therefore, it was necessary to modify the expressions for k_{IC} and k_{ST} for the purpose of explicit use in these expressions of the wave functions obtained as a result of quantum-chemical calculations.

Equation (6) was modified to have the following form [35]:

$$k_{pq}(\Psi_p \longrightarrow \Psi_q) = k_{pq}^{(1)} \Omega_{pq}, \quad (9)$$

where $\Omega_{pq} = N_{CH} \sum_{\alpha}^{N_{CH}} |\omega_{pq}^{\alpha}|^2$,

$$\omega_{pq}^{\alpha} = \sum_{ik,\,il} A_{ik}^p A_{il}^q \times (c_{ks}c_{ls} + c_{kx}c_{lx} + c_{ky}c_{ly} + c_{kz}c_{lz} + c_{kH}c_{lH})_\alpha - \sum_{ik,\,jk} A_{ik}^p A_{jk}^q (c_{is}c_{js} + c_{ix}c_{jx} + c_{iy}c_{jy} + c_{iz}c_{jz} + c_{iH}c_{jH})_\alpha + \sum_{ik} A_{ik}^p A_{ik}^q (c_{ks}^2 + c_{kx}^2 + c_{ky}^2 + c_{kz}^2 + c_{kH}^2 - c_{is}^2 - c_{ix}^2 - c_{iy}^2 - c_{iz}^2 - c_{iH}^2)_\alpha.$$

Here, c_{is}, c_{ix}, c_{iy}, c_{iz}, c_{iH} are the coefficients of the expansion of ith molecular orbital in the 2s, $2p_x$, $2p_y$, $2p_z$, and 1s atomic orbitals of the carbon and hydrogen atoms forming the C–H bond; $k_{pq}^{(1)}$ is defined by Eq. (6).

To calculate the values of $k_{pq}^{(1)}$ using a computer program, the following approximation was obtained:

$$k_{pq}^{(1)} = E_{pq}^{-2} 10^{(14 - E_{pq}/5)}, \quad (10)$$

where E_{pq} is in 10^3 cm^{-1} (if $E_{pq} < 10^3$ cm^{-1}, it is assumed that $E_{pq} = 10^3$ cm^{-1}). Approximation (5) permits modeling the known dependence $k_{pq}^{(1)}$ (E_{pq}) in the range $5 \times 10^3 < E_{pq} < 3 \times 10^4$ cm^{-1} with an accuracy of 5%.

In our works [36–40], we developed an algorithm for calculation of the matrix elements $\langle S(\pi\pi^*) | H_{SO} | T(\pi\pi^*) \rangle$ with allowance for all multicen-

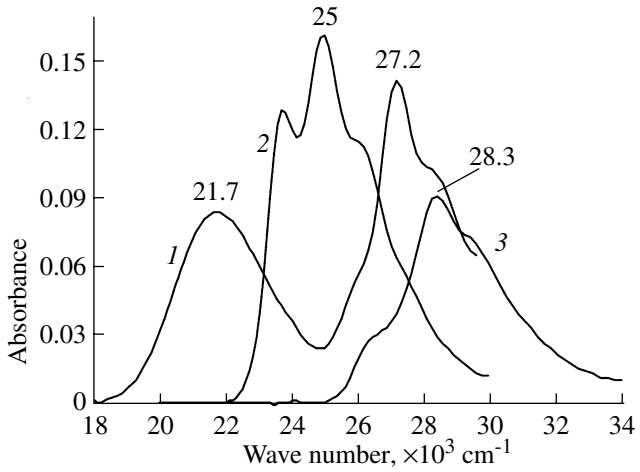

Fig. 2. Absorption spectra of (*1*) 9-DTAA, (*2*) 9-AA, and (*3*) acridine.

tered integrals calculated in the basis of the Gaussian atomic functions and created programs to provide for complete calculation of the corresponding matrix elements of the one-electron operator of spin–orbit coupling. This permitted quantitative estimation of k_{ST} for any type of interacting states in molecules of any spatial structure (including molecular complexes). Modification of the expressions for determination of the intersystem crossing and internal conversion rate constants involves calculation of electronic matrix elements and retains the estimate of the vibrational factors (Franck–Condon integrals) suggested earlier [29–32].

Thus, the software package developed permits calculation of the energy of molecular orbitals, the energy of singlet and triplet electronically excited states, the oscillator strength and polarization of electronic transitions, the distribution of electronic density on atoms and bonds of a molecule, the dipole moments in the ground and excited states, and the rate constants for nonradiative processes.

RESULTS AND DISCUSSION

Spectral-and-Luminescent Properties

Figure 2 shows the long-wavelength bands of the absorption spectra of ethanolic solutions of the test compounds (for 9-DTAA, two bands are shown). It can be seen that the long-wavelength band of acridine is weakly structured and has a maximum at 28 300 cm^{-1}. The long-wavelength bands of 9-AA and 9-DTAA are shifted to the red side with respect to the corresponding band of acridine and have maximums at 25 000 and 21 700 cm^{-1}, respectively; the long-wavelength band of 9-AA is also structured, in contrast to the broad unstructured band of 9-DTAA.

Table 1 presents the spectral characteristics of the acridine compounds in ethanol, weakly polar ethyl acetate, nonpolar carbon tetrachloride or cyclohexane, and ethanol with HCl admixtures.

It can be seen from Table 1 that the long-wavelength absorption band of acridine does not experience the solvatochromic effect, whereas the corresponding bands of 9-AA and 9-DTAA exhibit a small bathochromic shift upon replacement of a nonpolar solvent with ethanol.

The position of the fluorescence spectral bands is more sensitive to the solvent nature. For example, the fluorescence band of 9-AA exhibits a small long-wavelength shift on passing from nonpolar cyclohexane to more polar ethyl acetate and ethanol, with the same position of the fluorescence maximum in ethyl acetate and much more polar ethanol. This is presumably due

Table 1. Spectral and luminescent characteristics of acridine, 9-aminoacridine, and 2,7-dimethyl-9-ditolylaminoacridine in different solvents

Compound	Solvent	ν_{abs}, cm^{-1}	ν_{ex}, nm	ν_{fl}, m^{-1}	φ_{fl}	$\Delta\nu_{st}$, cm^{-1}
Acridine	Ethanol	28400	352	24100	0.03	4300
	Ethyl acetate	28400	352	не флуоресцирует@	–	–
	Cyclohexane	28200	352	не флуоресцирует@	–	–
Acridine cation	Ethanol + HCl	~25000		20800	0.27	4200
9-AA	Ethanol	25000	400	21800	0.61	3200
	Ethyl acetate	25000	400	21400	0.18	3600
	Cyclohexane	25800	400	22300	0.3	3500
9-DTAA	Ethanol	21700	460	16400	0.01	5300
	Ethyl acetate	22400	440	17800	0.14	4600
	CCl_4	22100	436	19300	0.36	2800
9-DTAA cation	Ethanol + HCl	18500	540	не флуоресцирует@	~0	–

Notes: ν_{abs} is the position of the maximum of the long-wavelength absorption band, ν_{fl} is the position of the fluorescence maximum, $\Delta\nu_{st}$ is the Stokes shift, φ_{fl} is the fluorescence quantum yield, and λ_{ex} is the fluorescence excitation wavelength.

to the fact that specific interactions between molecules of 9-AA and solvent molecules take place in ethanol.

Fluorescence of 9-DTAA, unlike the case of 9-AA, exhibits more significant changes on passing to more polar solvents. For this compound, a positive solvatofluorochromic effect is observed, with a red shift of the fluorescence spectra by more than 100 nm, which we also noted earlier [16].

The emissive power of compounds depends on both the structure of their molecules and the solvent nature. Measurements have shown that acridine fluorescence in ethanol has a very low intensity (fluorescence quantum yield $\varphi_{fl} = 0.03$), in agreement with the published data [19] ($\varphi_{fl} = 0.03$ in methanol). In nonpolar solvents, fluorescence of acridine was not detected. 9-Aminoacridine exhibits strong fluorescence in ethanol ($\varphi_{fl} = 0.61$) and weaker fluorescence in ethyl acetate ($\varphi_{fl} = 0.18$) and nonpolar cyclohexane. 2,7-Dimethyl-9-ditolylaminoacridine weakly fluoresces in ethanol and has quite strong fluorescence in nonpolar solvents ($\varphi_{fl} = 0.36$).

As noted above, the presence of the nitrogen atom in the acridine cycle permits the formation of protonated forms in acidic media. However, it turned out that the test compounds significantly differ in their behavior in acid solutions.

(1) The change in the absorption spectrum of acridine in acidified solutions is very specific. Along with the appearance of the band at the long-wavelength edge of the acridine absorption spectrum in the region of 400 nm, a rise in the intensity of the principal acridine band (~350 nm, Fig. 3a) is observed well, a situation that rarely happens in studies of the ion-neutral equilibrium of organic compounds in solutions. Similar results are reported in [24, 41]. The cationic form of acridine, unlike the neutral form, exhibits quite strong fluorescence. Even at a hydrochloric acid concentration of 10^{-5} mol l^{-1} in the solution, strong fluorescence at 479 nm is observed along with weak fluorescence at 415 nm, which belongs to the neutral form of acridine.

Figure 3b shows the fluorescence spectra of acridine and its protonated form. The acridine cation produces stronger fluorescence than the neutral form (quantum yield is 0.27).

(2) The behavior of 9-AA in acid solutions is different. Neither change in the shift nor deformation of the absorption and fluorescence spectra is observed at hydrochloric acid concentrations up to 1 mol l^{-1} in the solution. The intensity of the fluorescence spectra changes within ±10% without a tendency toward an increase (decrease) with an increase in the acid concentration. Similar results were reported by Oliveira et al. [42], who stated that the neutral form and the cation of 9-AA lie practically in the same region and their fluorescence quantum yields in methanol are close in value (0.45 and 0.56, respectively).

(3) The 9-DTAA molecule is readily protonated with hydrochloric acid, and all the molecules at an acid concentration of 10^{-1} mol l^{-1} are converted into the cation form, which has a well-defined absorption spectrum (Fig. 4). As shown above, 9-DTAA extremely weakly fluoresces in ethanol. We fail to detect the fluorescence of its protonated form under the given conditions.

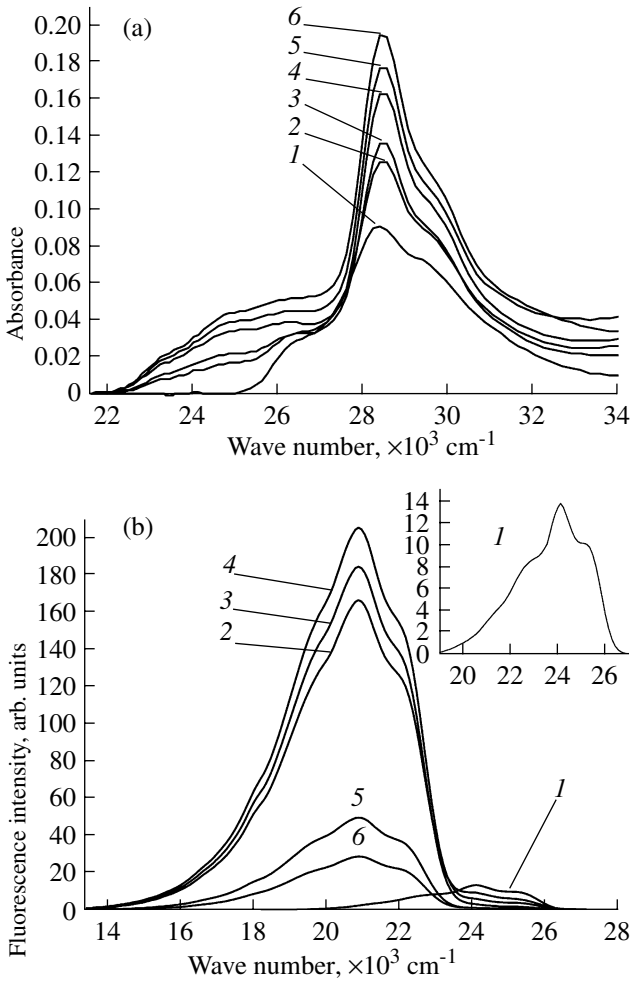

Fig. 3. Dependence of the (a) absorption and (b) fluorescence spectra of acridine in ethanol on the HCl concentration: (*1*) 0, (*2*) 10^{-5}, (*3*) 10^{-4}, (*4*) 10^{-3}, (*5*) 10^{-2}, and (*6*) 10^{-1} mol l^{-1}.

Results of Quantum-Chemical Calculations

To perform quantum-chemical calculations, it is necessary to preset the molecular geometry. For this purpose, the standard AM1 and PM3 methods were used in this work. It was shown that acridine and aminoacridine have the planar structure; the plane of the Ph–N–Ph bonds in 9-DTAA is located at an almost right angle to the plane of the acridyl cycle, whereas the phenyl rings of the substituent make angles of 21° and 43° with the Ph–N–Ph plane. However, these results are for the geometry at which the Ph–N–Ph plane is turned by 30° with respect to the acridyl cycle, since it is for this structure that good conjugation of the fragments takes place and the discrepancy between the S_0-S_1 tran-

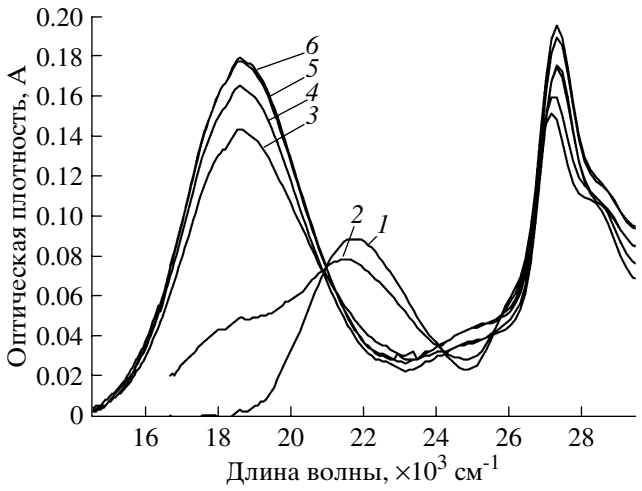

Fig. 4. Dependence of the absorption spectrum of 9-DTAA in ethanol on the HCl concentration: (*1*) 0, (*2*) 10^{-5}, (*3*) 10^{-4}, (*4*) 10^{-3}, (*5*) 10^{-2}, and (*6*) 10^{-1} mol l^{-1}.

Key: 1. Wave number @ 10@–3, cm@–1; 2. Absorbance

sition energy and the position of the long-wavelength absorption band is the least. Studies have shown that this angle slightly increases to 46° upon the conversion of the 9-DTAA molecule to the cationic form.

Table 2 presents calculated data on the energies of some singlet states of the test molecules; their orbital nature; the oscillator strengths for the corresponding transitions; and the fluorescence quantum yields φ_{calcd} calculated by the expression $\varphi = k_r/k_r + k_{IC} + k_{ST}$, where k_r, k_{IC}, and k_{ST} are the radiative decay, internal conversion, and intersystem crossing rate constants, respectively.

It can be seen from Table 2 that there is correlation the position of the S_0-S_1 transition and the long-wavelength absorption band of the corresponding molecules, as well as agreement between the calculated and experimental values of the fluorescence quantum yields.

Figure 5 shows the energy diagram for electronically excited states of acridine, 9-AA, and 9-DTAA, as well as the rates of internal conversion, intersystem crossing, and radiative transition.

Let us consider in detail the spectral and luminescent properties of acridine. Parameterization of the method used was based on the experimental data on the spectra of organic compounds in hydrocarbon solutions [27]; therefore, the calculation results should well reproduce the experimental spectral data in "inert" and weakly polar solvents. Since acridine is an azaderivative of anthracene and the π systems of acridine and anthracene are isoelectronic, the structures of the lower excited states of acridine and anthracene are kindred. Recall that the S_1 state of anthracene is a well-resolved ππ* state of the B_{2u} symmetry (according to Platt's classification, L_a) and the S_2 state is a weakly resolved ππ* state with the B_{3u} symmetry (L_b). In acridine, the *n*π* state appears, which is associated to excitation of the lone electron pair of the nitrogen atom. The energy gap between the singlet and triplet states of the *n*π* type is usually 2000–3000 cm^{-1}.

From the data presented in Table 2 and Fig. 5, it can be seen that the first three singlet states of acridine are practically degenerate in energy and are arranged in the order: L_a, *n*π*, and L_b. Of these states, the most optically active state is S_1 of the ππ* orbital nature with an oscillator strength of the $S_0 \longrightarrow S_1$ electronic transition of 0.24. The S_1 state is adjacent to the closely located $T_3(n\pi^*)$ state. The calculation of the deactivation constants of the excited state has shown that the main decay pathway of the S_1 state is $S_1 \longrightarrow T_3$ intersystem crossing ($k_{ST} = 1.5 \times 10^{11}$ s^{-1}). As a consequence, the theoretically calculated fluorescence quantum yield of acridine is low, ~10^{-4}. Hence, in the absence of specific interactions in inert, weakly polar solvents, the acridine molecule should not fluoresce, which is in fact the case observed experimentally. Note that the deactivation rate constant for the S_1 state via intersystem crossing is much higher than the rate constant for $S_1 \longrightarrow S_0$ internal conversion; that is, the Ermolaev–Sveshnikova rule is obeyed. The orbital nature and the relative position of the lower states of different multiplicity correspond to the fourth type of the spectral and luminescent systematization [13–15].

There are a number of works devoted to photophysics of acridine [43–45]. The results of theoretical quantum-chemical calculations of the electronic states are presented in [44, 45]. Rak and Blazejowski [44] performed INDO calculations. Rubio-Pons et al. [45] used the ab initio approach and the second-order perturbation theory. The energies of the singlet and triplet states, the oscillator strengths, and the rate constants for radiative transitions were calculated. However, no attempt to theoretically estimate the rate constants for nonradiative deactivation (including singlet–triplet conversion) was made in the cited works.

The energies calculated in [44, 45] for the three lower singlet states agree quite well with the absorption spectra, but they are arranged in the following order: *n*π*, L_b, and L_a. A similar scheme of the electronic states was considered by Diverdi and Topp [43] upon interpretation of the fluorescent properties of acridine in different solvents. The low experimental quantum yield of acridine fluorescence (~10^{-4}) was explained by a high rate constant for the $S_{n\pi^*} \longrightarrow T_{\pi\pi^*}$ conversion. It was assumed that El-Sayed's rule is obeyed for this conversion pathway [33]. However, it should be borne in mind that this rule was developed for the $S_{n\pi^*} \rightleftharpoons T(L_a)$ conversion. Indeed, our estimates show that the matrix elements $\langle S_{n\pi^*}|H_{SO}|T(L_a)\rangle$ and $\langle S(L_a)|H_{SO}|T_{n\pi^*}\rangle$ have values of ~9.5 cm^{-1}. According to Eq. (7), the singlet–triplet conversion rate constant depends on both the value of the matrix element and the corresponding Franck–Condon factor, whose value rapidly decreases with an

increase in the energy gap between the interacting states. The T_1 state of acridine is an L_a state. Since the energy interval between the $S_{n\pi^*}$- and $T(L_a)$ states is about 10000 cm^{-1}, the rate constant for the $S_{n\pi^*} \longrightarrow T(L_a)$ conversion will be about 10^8 s^{-1}, despite the high value of the matrix element. The theoretical fluorescence quantum yield in this case will be ~0.01, which disagrees with the experimental value of this fluorescence characteristic of acridine in nonpolar solutions. Nevertheless, it was this (erroneous) explanation for the low fluorescence quantum yield of acridine in nonpolar solvents that was given in [43].

The following arrangement of the triplet states was obtained in [45]: $T(L_a)$, $T_{n\pi^*}$, and $T(L_b)$. In this case, the $S_{n\pi^*} \longrightarrow T(L_b)$ conversion was assumed to be the main nonradiative deactivation pathway. Our calculations show that $\langle S_{n\pi^*}|H_{SO}|T(L_b)\rangle \approx 0.2$ cm^{-1}, a value that is associated to the configurational structure of the wave function of L_b states. With such a value of the matrix element, even in the case of almost degenerated $S_{n\pi^*}$- and $T(L_b)$states (as in [45]), the corresponding rate constant will be about 10^8 s^{-1} again, which does not permit explanation for the experimental data on the fluorescence quantum yield of acridine in nonpolar solutions.

Thus, the lack of quantitative determination of the $S \longrightarrow T$ conversion rate constants in [43, 45] leads to erroneous conclusions about the energy diagram of the singlet and triplet states and the efficiency of photoprocesses in the acridine molecule. At the same time, the method for calculating the electronic states and the procedures for quantitative determination of the rate constants for all photophysical processes, which we used, permitted complete description of acridine photophysics in accordance with the set of the experimental data.

The amino group as an electron-donating substituent decreases the energy of the $S_1(\pi\pi^*)$ state of 9-AA and increases the energy of the $T_3(n\pi)$ state, leading to the energetic inversion of these states relative to the acridine molecule. Deactivation of the S_1 state proceeds with comparable rate constants via the radiative pathway ($k_r = 1.5 \times 10^8$ s^{-1}) and intersystem crossing ($k_{ST} = 1.9 \times 10^8$ s^{-1}). The theoretically calculated quantum yield of 9-AA fluorescence was found to be 0.44, which is close to the experimental value in ethanolic solutions. The value of φ_{calc} is given without allowance for the interaction of S_1 with T_3, whose energy is slightly higher (by 1000 cm^{-1}) than that of the S_1 state. However, the coupling of these states is strong, the rate constant $k_{ST} = 4.2 \times 10^{11}$ s^{-1} (Fig. 5). It is likely that this interaction is not critical in protic ethanol owing to the formation of a hydrogen bond of the solvent with the lone electron pair of the acridine nitrogen atom. Since 9-AA fluoresces very weakly in nonpolar cyclohexane, it may be concluded that this interaction has the determining role in the deactivation of excitation and intersystem crossing becomes the main decay pathway for the S_1 state.

Table 2. Results of quantum-chemical calculations

State (orbital nature)	Energy, cm^{-1} (wavelength of S_0–S_n transition)	Oscillator strength	φ_{calc} (φ_{exp})
Acridine			
$S_1(\pi\pi^a)$	28861 (28400)[a]	0.24	10^{-4} (~0)
$S_2(n\pi^a)$	28966	0.005	
$S_3(\pi\pi^a)$	29294	0.075	
$S_7(\pi\pi^a)$	40850	2.3	
Acridine cation			
$S_1(\pi\pi^a)$	26471 (26500)[a]	0.15	0.24 (0.27)
$S_2(\pi\pi^a)$	29404	0.19	
$S_3(\pi\pi^a)$	33369	0.21	
$S_6(\pi\pi^a)$	40000	1.44	
9-AA			
$S_1(\pi\pi^a)$	26469 (25500)[a]	0.3	0.44 (0.18, 0.61)
$S_2(n\pi^a)$	29479	0.004	
$S_3(\pi\pi^a)$	29597	0.0047	
$S_7(\pi\pi^a)$	39906	1.41	
9-AA cation			
$S_1(\pi\pi^a)$	26717 (26700)	0.22	0.027
$S_2(n\pi^a)$	31164	0.063	
$S_3(\pi\pi^a)$	34982	0.23	
$S_4(\pi\pi^a)$	38736	0.048	
$S_7(\pi\pi^a)$	40358	1.59	
9-DTAA			
$S_1(\pi\pi^a)$	22733 (22500)[a]	0.01	0.54 (0.34)
$S_2(n\pi^a)$	27443	0.31	
$S_3(\pi\pi^a)$	28597	0.084	
$S_5(\pi\pi^a)$	30172	0.17	
9-DTAA cation			
$S_1(\pi\pi^a)$	18700 (18500)*	0.19	0.042 (~0)
$S_2(n\pi^a)$	27000	0.16	
$S_3(\pi\pi^a)$	28324	0.03	
$S_4(\pi\pi^a)$	29345	0.05	
$S_6(\pi\pi^a)(\sigma^a)$	33554	0.18	

[a] The experimental position of the maximum of the long-wavelength absorption band.

In the 9-DTAA molecule, the energy of the $S_1(\pi\pi^*)$ state further decreases because of the electron-donating effect of the ditolylamine substituent. The S_1 state decays with almost the same probability via three pathways: radiative deactivation ($k_r = 3.7 \times 10^6$ s^{-1}), internal conversion ($k_{IC} = 3.7 \times 10^6$ s^{-1}), and intersystem crossing ($k_{ST} = 1.4 \times 10^6$ s^{-1}). As a result, the calculated fluorescence quantum yield of 9-DTAA is 0.54.

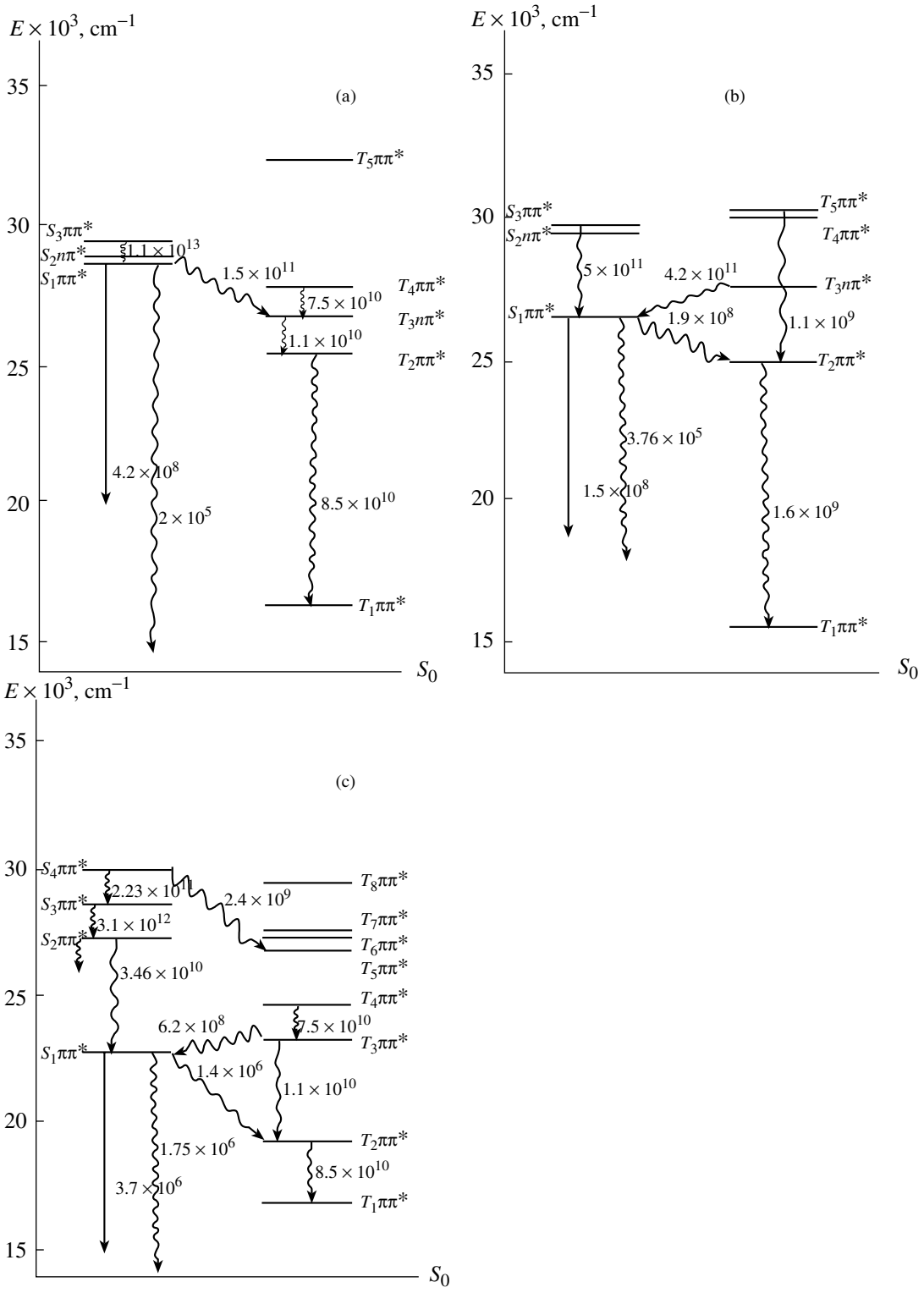

Fig. 5. Schemes of the electronically excited states and photophysical processes of (a) acridine, (b) 9-aminoacridine, and (c) 2,7-dimethyl-9-ditolylaminoacridine molecules.

Table 3 presents the calculated values of the dipole moments and the effective charges on nitrogen atoms and fragments of the molecules in the ground and excited (S_1) states.

The dipole moments of the ground-state acridine and 9-AA molecules are 3.4 and 5.8 D, respectively (the experimental values are 2.99 and 5.23 D [46]). In the excited state, the dipole moments of acridine and

Table 3. Effective charges on the nitrogen atoms and fragments of molecules, and the dipole moments in the S_0 and S_1 states

Fragment	Acridine		9-AA		9-DTAA	
	S_0	S_1	S_0	S_1	S_0	S_1
N(Ac)	–0.467	–0.426	–0.530	–0.408	–0.481	–0.545
N(Am)	–	–	–0.344	–0.331	–0.192	–0.028
Acridyl	–	–	0.021	0.007	0.020	–0.586
NR_2 group	–	–	–0.021	–0.007	–0.020	0.586
Dipole moment, D	3.4	2.7	5.8	4.2	3.9	12.2

Notes: N(Ac) is the nitrogen atom in the acridine cycle, N(Am) is the nitrogen atom of the amino group or the ditolylamine moiety, and R is the tolyl moiety.

9-AA are lower, 2.7 and 4.25 D, respectively. This is due to a more uniform distribution of the electron density in these molecules in the S_1 state: the negative charge on the nitrogen atom of the acridine cycle decreases (Table 3). The solvatochromic effect of acridine is not expressed, probably, owing to a smaller change in the dipole moment ($\Delta\mu = 0.7$) upon excitation to the S_1 state. For 9-AA, a small red solvatochromic shift is observed, which corresponds to an increase of the dipole moment in the dipole state and does not coincide with the calculation results. A similar result was obtained for 9-AA in [46]. The excited-state dipole moment calculated by the Pople–Pariser–Parr method is 4.59 D, whereas that obtained from the experimental data on the basis of Bakhshiev's formula is 8.7 D. This discrepancy between the theoretical and experimental values of the dipole moment of 9-AA in the excited state is explained by strong specific interactions between dye molecules and molecules of polar solvents.

In the 9-DTAA molecule, excitation results in a large increase in the dipole moment, from 3.9 to 12.2 D. These values obtained by the quantum-chemical calculation are close to those obtained in [16] on the basis of the spectroscopic data (μ_{S0} = 2 D, μ_{S1}=12 D). Such a strong change in the dipole moment upon excitation to the S_1 state is due to significant redistribution of electron density (~0.6 e) from the ditolylamine to the acridine fragment (Table 3). Note that the change on the nitrogen atoms of these moieties is ~30% of the total electron density redistribution between the fragments. On the basis of the electron density redistribution and the change in the dipole moment, we can conclude that the long-wavelength absorption band of 9-DTAA is a charge-transfer band in character. This conclusion is confirmed by the molecular structure of the singly excited configuration, which makes the main contribution to the formation of the S_1 wave function of the molecule. This configuration involves occupied MO localized on the ditolylamine fragment and unoccupied MO localized on the acridine fragment. The photophysical characteristics of such charge-transfer states of aryl derivatives of aromatic amines were studied in [47].

The energies of the excited states and the constants of the photophysical processes of the molecules protonated at the nitrogen atom in the acridine cycle were calculated. For such structures, the calculation of the energies of the excited states shows good agreement with the experimental absorption spectra (Table 2). It follows from the calculation results that protonation generally leads to a decrease in the energy of the S_1 state as compared to that of the neutral forms and to disappearance of the neighboring $n\pi^*$ states. For the acridine cation, the lowest singlet and triplet states are both of the $\pi\pi^*$-orbital nature. The rate of singlet–triplet conversion to lower-lying triplet states of the same orbital nature decreases by several orders of magnitude, thereby leading to activation of fluorescence of the acridine cation.

In the Experimental section, it has been noted that, absorption intensity at the main band grows upon acridine protonation. It can be seen from the calculation results (Table 2) that the cation in this spectral region has two allowed transitions, S_2 and S_3, with oscillator strengths of 0.19 and 0.21, respectively.

The energy of the S_0-S_1 transition in the 9-AA cation (26 717 cm^{-1}) practically coincides with that of the neutral form (26 469 cm^{-1}, Table 2). It becomes clear why changes in the absorption and fluorescence spectra of 9-AA in acid media were experimentally undetectable. The absorption by the cation practically coincides with that of the neutral form; they have similar oscillator strengths as well (0.22 and 0.3, respectively).

The $S_1(\pi\pi^*)$ state of the 9-AA cation is very close to the $T_2(\pi\pi^*)$ state (E = 26 512 cm^{-1}), which results in the fact that the rate of singlet–triplet conversion via this channel ($k_{ST} = 4 \times 10^9$ s^{-1}) is much higher than the rate of radiative decay ($k_r = 10^8$ s^{-1}), and the calculated fluorescence quantum yield is low (0.027). However, since 9-AA exhibits quite strong fluorescence in acid media, the actual position of the T_2 level is most likely so high that there is no strong coupling between the levels.

For the 9-DTAA cation, the main decay pathway of the $S_1(\pi\pi^*)$ state is the singlet–triplet conversion (k_{ST} = 10^9 s^{-1}) to the neighboring triplet $T_2(\pi\pi^*)$, whose rate is much higher than the rate of radiative decay (k_r =

4.6×10^7 s^{-1}). The theoretically calculated fluorescence quantum yield is low, 0.042. This explains the absence of fluorescence by the 9-DTAA cation.

CONCLUSIONS

In summary, the results obtained show that the semiempirical method of calculation of the spectral characteristics of acridine and its 9-substituted derivatives (9-AA and 9-DTAA), which was used in this work, gives sufficiently good description of radiative and nonradiative processes in these molecules. Although the experimental data on the constants of photophysical processes in acridine and 9-AA have been discussed earlier [20, 21], these constants seem to be analytically calculated for the first time.

Note that the results obtained in this work by the INDO method on the energy levels of acridine are close to the ab initio calculation results [45].

On the basis of the calculated and experimental data, a scheme of deactivation processes occurring in the 9-DTAA dye molecule is presented. of The S_1 state decays with almost equal probabilities via three pathways: radiative deactivation ($k_r = 3.7 \times 10^6$ s^{-1}), internal conversion ($k_{IC} = 3.7 \times 10^6$ s^{-1}), and intersystem crossing ($k_{ST} = 1.4 \times 10^6$ s^{-1}). It was shown that the lack of fluorescence ($k_r = 4.6 \times 10^7$ s^{-1}) from the 9-DTAA cation is due to suppression of fluorescence by the intersystem crossing process, which occurs with a much higher probability ($k_{ST} = 10^9$ s^{-1}). The calculated values of the dipole moments in the ground and excited states agree well with the experimentally measured dipole moments.

Based on the foregoing, we conclude that the software program used for calculations in this work can be successfully applied to the calculation of the photophysical characteristics of other 9-substituted acridines.

REFERENCES

1. Silva, A.P. and Gunarate, H.Q.N., *Chem. Rev.,* 1997, vol. 97, p. 1515.
2. Plotnikov, V.G., Sazhnikov, A.V., and Alfimov, M.V., *Khim. Vys. Energ.*, 2007, vol. 41, no. 5, p. 1 [*High Energy Chem.*, 2007, vol. 41, no. 5, p. 299].
3. Eggins, B.R., *Chemical Sensors and Biosensors*, New York: Wiley, 1997.
4. Bogenkov, V.E. and Sergeev, G.B., *Usp. Khim.*, 2007, vol. 76, p. 1084.
5. Bochenkov, V.E. and Sergeev, G.B., *Adv. Coll. Int. Sci.*, 2005, vol. 116, p. 245.
6. Kohl, D., *J. Phys. D: Appl. Phys.*, 2001, vol. 34, p. 125.
7. Docquier, N. and Candel, S., *Prog. Energy Combust. Sci.*, 2002, vol. 28, p. 107.
8. Ampuero, S. and Bosset, J.O., *Sens. Actuators, B,* 2003, vol. 94, p. 1.
9. Nicolas-Delarnot, D. and Poncin-Epaillard, F., *Anal. Chim. Acta*, 2003, vol. 475, p. 1.
10. Haes, A.J. and Van Duyne, R.P., *Anal. Bioanal. Chem.*, 2004, vol. 379, p. 920.
11. Timmer, Olthuis, W. and Van den Berg, A., *Sens. Actuators, B*, 2005, vol. 107, p. 666.
12. Rin, J., Maroto, A., and Rius, F.X., *Talanta*, 2006, vol. 69, p. 288.
13. Pereira, R.V., Ferreira, A.P.G., and Gehlen, M.H., *J. Phys. Chem. A*, 2005, vol. 109, p. 5978.
14. Plotnikov, V.G., *Usp. Khim.*, 1980, vol. 49, no. 2, p. 327.
15. Nurmukhametov, R.N., *Pogloshchenie i lyuminestsentsiya aromaticheskikh soedinenii* (Adsorption and Luminescence of Organic Compounds), Moscow: Khimiya, 1971.
16. Sazhnikov, V.A., Khlebunov, A.A., and Alfimov, M.V., *Khim. Vys. Energ.*, 2007, vol. 41, no. 1, p. 28 [*High Energy Chem.*, 2007, vol. 41, no. 1, p. 25].
17. Parker, C.A., *Photoluminescence of Solutions*, Amsterdam: Elsevier, 1968.
18. Terenin, A.N., *Fotonika molekul krasitelei* (Photonics of Dye Molecules), Leningrad: Nauka, 1967.
19. Koichi, K., Kunihiko, K., Akihiko, K., Koji, U., Hiroshi, K, *J. Phys. Chem.*, 1985, vol. 89, p. 868.
20. Kunihiko, K., Koichi, K., Sada-Aki, Y., Koji, U., Yoshlyuki, N., and Kokubun, H., *J. Phys.Chem.*, 1981, vol. 85, p. 1291.
21. Kunihiko, K., Koichi, K., Yoshlyuki, N., and Kokubun, H., *J. Phys.Chem.*, 1981, vol. 85, p. 4148.
22. Kunihiko, K., Koichi, K., Koji, U., Sada-Aki, Y., and Kokubun, H., *J. Phys. Chem.*, 1982, vol. 86, p. 4733.
23. Pines, E., Huppert, D., Gutman, M., Nachliel, N., and Fishman, M., *J. Phys.Chem.*, 1986, vol. 90, p. 6366.
24. Tomasz, P., Bronislaw, M., and Gordon, L.H., *J. Photochem. Photobiol., A: Chem.*, 2007, vol. 150, p. 21.
25. Sundstrom, V., Rentzepis, P.M., and Lim, E.C., *J. Chem. Phys.*, 1977, vol. 66, no. 10, p. 4287.
26. Jones, G., Jackson, W.R., and Chol-You, C., *J. Phys. Chem.*, 1985, vol. 89, p. 294.
27. Artyukhov, V.Ya. and Galeeva, A.I., *Izv. Vyssh. Uchebn. Zaved., Fiz.*, 1986, no. 11, p. 96.
28. Maier, G.V., Artyukhov, V.Ya., and Bazyl', O.K., *Elektronno-vozbuzhdennye sostoyaniya i fotokhimiya organicheskikh soedinenii* (Electronically Excited States in Photochemistry of Organic Compounds), Novosibirsk: Nauka, 1997.
29. Plotnikov, V.G. and Dolgikh, V.A., *Opt. Spektrosk.*, 1977, vol. 43, no. 5, p. 882.
30. Plotnikov, V.G., The Nature of Electronically Excited States and Spectral-and-Luminescence Properties of Polyatomic Molecules, *Doctoral (Phys.-Math.) Dissertation*, Obninsk: Karpov Inst. of Physical Chemistry, 1980.
31. Plotnikov, V.G., Dolgikh, B.A., and Komarov, V.M., *Opt. Spektrosk.*, 1977, vol. 43, no. 6, p. 1972.
32. Plotnikov, V.G., *Int. J. Quantum Chem.*, 1979, vol. 16, p. 527.
33. El-Sayed, M.A., *J. Chem. Phys.*, 1963, vol. 38, no. 18, p. 2834.
34. Hameka, H. and Oosterhoff, L., *Mol. Phys.*, 1958, vol. 1, p. 358.

35. Artyukhov, V.Ya., Galeeva, A.I., Maier, G.V., and Ponomarev, V.V., *Opt. Spektrosk.*, 1997, vol. 82, no. 4, p. 563 [*Opt. Spectrosc.* 1997, vol. 82, no. 4, p.].
36. Artyukhov, V.Ya. and Maier, G.V., *Opt. Spektrosk.*, 1988, vol. 64, no. 5, p. 1018.
37. Maier, G.V., Artyukhov, V.Ya., and Karypov, A.V., *Opt. Spektrosk.*, 1989, vol. 66, no. 4, p. 823.
38. Maier, G.V., *Fotofizicheskie protsessy i generatsionnaya sposobnost' organicheskikh soedinenii* (Photophysical Processes and Lasing Ability of Organic Compounds), Tomsk: Tomsk. Gos. Univ., 1992.
39. Artyukhov, V.Ya. and Pomogaev, V.A., *Izv. Vyssh. Uchebn. Zaved., Fiz.*, 2000, vol. 43, no. 7, p. 68.
40. Pomogaev, V.A. and Artyukhov, V.Ya., *Zh. Prikl. Spectrosk.*, 2001, vol. 68, no. 2, p. 192.
41. Ryan, E.T., Xiang, T., Johnston, K.P., and Fox, M.A., *J. Phys.Chem.*, 1997, vol. 101, p. 1827.
42. Oliveira, H.P.M., Camargo, A.J., Macedo, L.G.M., Gehlen, M.H., and Silva, A.B.F., *J. Mol. Struct. (Theochem)*, 2004, vol. 674, p. 215.
43. Diverdi, L.A. and Topp, M.R., *J. Phys. Chem.*, 1983, vol. 88, p. 3447.
44. Rak, J. and Blazejowski, J., *J. Photochem. Photobiol, A: Chem.*, 1992, vol. 67, p. 287.
45. Rubio-Pons, O., Serrano-Andres, L., and Merchan, M., *J. Phys. Chem. A*, 2001, vol. 105, p. 9664.
46. Aaron, J.J. and Maafi, M., *Spectrochim. Acta*, 1995, vol. 51A, no. 4, p. 603.
47. Herbich, J. and Kapturkiewicz, A., *J. Am. Chem. Soc.*, 1998, vol. 120, p. 1014.

SPELL: 1. Vys